XLVI CILAMCE
VITÓRIA - ES - BRAZIL - 2025
XLVI IBERO-LATIN AMERICAN CONGRESS ON COMPUTATIONAL METHODS IN ENGENEERING

Mechanical Characterization of Breast Compression with Cancerous Tissue Using an Axisymmetric Numerical Model

William de A. Peters[1], Renato V. Linn[1], Branca F. de Oliveira[1], Mariana P. de Oliveira[1]

[1]*Graduate Program in Design (PGDesign), Federal University of Rio Grande do Sul*
Av. Osvaldo Aranha, 99, Porto Alegre, 90035-190, RS, Brazil
william.peters@ufrgs.br, renatolinn@ufrgs.br, branca@ufrgs.br, mariana.pohlmann@ufrgs.br

Abstract. Breast cancer is the leading cause of cancer-related deaths among women in Brazil and the second leading cause worldwide. Detecting the disease in its early stages is an effective way to increase survival rates. Ultrasound elastography is a non-invasive procedure, capable of providing data on tissue stiffness based on compression applied by an external force to the breast. Cancerous tissue is stiffer than the surrounding healthy tissue, and the nonlinear strain behavior of the compressed breast can be used to determine the nature of the inclusion using this approach. In this work, a numerical axisymmetric breast model is proposed with a simplified tissue distribution. The tissues were modeled as nonlinear elastic materials, and the breast model was compressed by a rigid spherical indenter to simulate the clinical elastography test, in which large strains and nonlinear geometric effects take place. The obtained results were compared with simplified theoretical analytical solutions for spherical indentation in a homogeneous material, as well as with results from other authors using different three-dimensional numerical models. As a result, the present simplified axisymmetric model shows good agreement in the mechanical characterization of the effect of cancerous inclusions on breast compression, enabling fast and parametric analysis.

Keywords: Biomechanics, Finite Element Analysis, Breast Cancer, Elasticity, Elastography

1 Introduction

Breast Cancer (BC) is the leading cause of cancer deaths among women in Brazil, being the second most prevalent (INCA [1]) as well as a global public health problem. Because of the late screening of the pathology, older women aged between 50-69 are the most affected, with mortality rates among 45% of cases (INCA [2]). One effective way to reduce this rate and having a good outcome in BC treatment is to ensure the early detection of the disease. The main methods for early identification of breast lesions are self-examination, mammography, and clinical analysis. However, to confirm the diagnosis, a biopsy is necessary. The procedure typically requires a large diameter needle and to be conducted under local anesthesia and image guidance, possibly causing hematoma, pain, and discomfort. However, other clinical medical tests can be considered in order to identify breast cancers, being the ultrasound breast elastography one of them.

Breast elastography is a noninvasive ultrasound technique that can provide both qualitative and quantitative data on tissue stiffness based on its displacement from a compression applied by an external force (Barr [3]). Introduced by Ophir et al. [4], it can obtain information about tissue mechanical properties through its deformation, which can help cancer diagnosis procedures (Sayed et al. [5]). As healthy tissues tend to be softer and expected to exhibit larger strain under the pressure of the ultrasound probe, malignant lesions, conversely, tend to deform less (da Rocha [6]). Therefore, it is possible to distinguish the nature of the inclusion based on the nonlinear mechanical behavior of the tissues under compression. Nevertheless, false negative results can occur and achieving quality images can be operator-dependent sensitive (Barr [7]). Hence, the mechanical characterization of breast under compression can help to improve detection and calibrate elastrography procedures (Kallel et al. [8]; Ophir et al. [9]).

The biomechanical Finite Element (FE) modeling of the breast tissues have been investigated over the last 20 years for all sorts of applications, such as biomechanical analysis (Chen et al. [10]), preoperative planning (Del Palomar et al. [11]), clinical tests (Ahangar Darband et al. [12]), etc. Thus, FE can be a useful tool to simulate and analyze the biomechanics of the breast in the context of elastography by helping to identify whether a lesion is benign or malignant. By means of determining the total displacement of the probe over the computational breast model, it is possible to quantify the force that needs to be applied to deform its tissues.

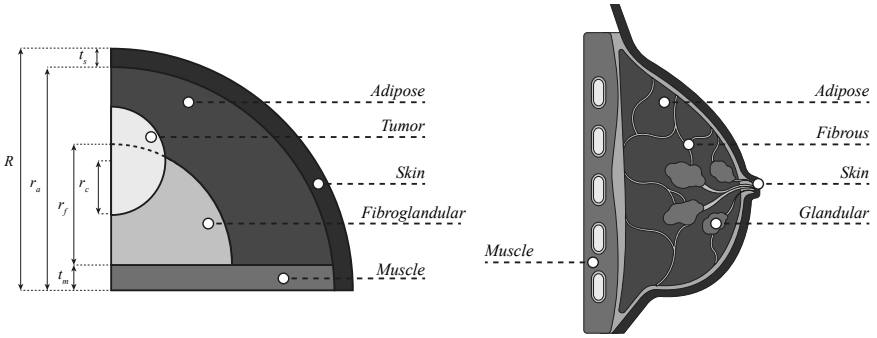


Figure 1. Simplified breast tissues model (left); illustration of the anatomy of the breast tissues (right).

Given the relevance of this subject, investigations on the elastography test in the context of FEA have already been carried out, taking into account three main aspects: the definition of breast geometry, tissue distribution, and constitutive relationship. In computational biomechanical studies, the breast can be represented by spherical or semi-spherical shapes (Naser et al. [13]), elastic layers (da Rocha [6]) or more complex models obtained from images, such as MR data. Regarding tissue distribution, the digital model can consist of a single homogeneous material (Naser et al. [13]), simplified layers (da Rocha [6]) or a more realistic distribution based on individual patient data (Chen et al. [10]). In order to carry out the analysis, constitutive relationships are usually elastic (da Rocha [6]) or hyperelastic (Naser et al. [13]).

In this work, a non-homogeneous axisymmetric biomechanical model for the breast is proposed. The skin, muscle, adipose and fibroglandular tissues were considered as distributed along axisymmetric layers inside an hemispherical shape. The breast composition in terms of fibroglandular and adipose tissue, defined as the breast density, is derived and analyses are parametrized in terms of such compositions. The consideration of cancerous tissue is performed by spherical inclusions with different sizes and stiffness on the biomechanical breast model. A finite strain elastic constitutive model is considered for all tissues. For modeling the elastography clinical procedure, the breast compression by an ultrasound probe is represented as indentation of the deformable breast by a rigid sphere. Following da Rocha [6], a simplified hemispherical shape assumption is considered for the probe geometry. An analytical homogeneous solution for the rigid indentation is presented and compared to the compression of the present numerical model.

2 Breast Biomechanical Model

An axisymmetric breast model is considered for this study with four different tissue: skin, adipose, fibroglandular and muscle, which is illustrated in Fig. 1. Defining the outer breast radius as R, muscle tissue thickness as t_m, skin thickness as t_s, fibroglandular and adipose tissue radius as r_f and r_a, respectively, the breast total volume V can be evaluated as an hemisphere, thus: $V = \frac{2}{3}\pi R^3$. The volume of fibroglandular tissue V_f and combined volume of fibroglandular and adipose tissue V_{f+a} for a healthy breast can be directly derived from geometry data as $V_f = \frac{2}{3}\pi r_f^3$ and $V_{f+a} = \frac{\pi}{3}\left(R - t_s - t_m\right)^2\left(2R + 2t_s + t_m\right)$. Such relations provide the geometrical and tissue distribution of the simplified breast model, which can be directly related to commonly obtained data such as breast volume or tissue fractions from computer tomography image. A commonly used parameter is the breast density ρ which is defined as the fraction of fibroglandular to adipose volume (Sak et al. [14]). Thus:

$$\rho = \frac{V_f}{V_{f+a}} = \frac{r_f^3}{\left(R - t_s - t_m\right)^2\left(R - t_s + t_m/2\right)}, \tag{1}$$

which can be used to derive the geometry in order to provide a given breast density. The tissue are modeled as elastic materials with finite strain, where (E_m, ν_m), (E_s, ν_s), (E_f, ν_f) and (E_a, ν_a) are the Young's modulus and Poisson's ratio for muscle, skin, fibroglandular and adipose tissue, respectively. The consideration of a cancerous inclusion into the breast is performed by including an elastic sphere with radius r_c at the center of the symmetry line with elastic properties (E_c, ν_c).

Table 1. Mechanical properties of the different breast tissues.

Tissue	r_c (mm)	E (kPa)	ν
Skin		1500	0.45
Adipose		15	0.45
Fibroglandular		30	0.45
Muscle		28	0.45
Tumor$(1,2,3)$	5(1), 15(2), 27.5(3)	33.904(1), 60(2),111.174(3),	0.45

2.1 Tissue Mechanical Properties

In this work, an elastic constitutive relationship was considered to model the tissues mechanical behavior considering large strains and nonlinear geometric effects. For characterizing the mechanical properties, the experimental data of Young's modulus E and Poisson's ratio ν provided by Nazri et al. [15], Said Camilleri et al. [16] and da Rocha [6] were considered in this work. Following da Rocha [6], in order to simulate different stiffness of tumors of benign and malignant nature, three distinct values of Young's modulus were considered, while three tumor sizes were used to represent its different stages: 10, 30, and 55 mm. The mechanical properties of the different breast tissues and tumor sizes are indicated in Table 1.

2.2 Breast Compression

A simplified hemispherical shape assumption with radius R_0 is considered for the probe geometry in this work and its indentation on the breast model is investigated. The finite strain analytical solution of a spherical indentation of an elastic sphere can be determined for an homogeneous material. The displacement along the axial direction δ is shown in Fig. 2 (left) and is related to the indenter radius R_0 and elastic sphere radius R through the relation (Argatov et al. [17]):

$$\frac{\delta}{R} = \left(\frac{3(1-\nu)\sqrt{\beta}F}{8R^2G}\right)^{2/3} + \frac{F}{8\pi R^2 G}\left(\frac{2}{3}(1-2\nu)^2 \ln\left(\frac{R^2G\beta}{3(1-\nu)F}\right) + C\right), \tag{2}$$

where $\beta = (R_0 + R)/R_0$, $C = C(\nu)$ is a function of ν and $G = E/2(1+\nu)$ is the shear modulus of the material. For an almost incompressible material in which $\nu \to 0.5$, $C \to -1.17706$ (Argatov et al. [17]). Therefore, Eq. (2) provides an analytical relation for the spherical indentation of a homogeneous elastic sphere. Since the considered breast model is not homogeneous, a shift from such analytical prevision is expected depending on the tissue proportion.

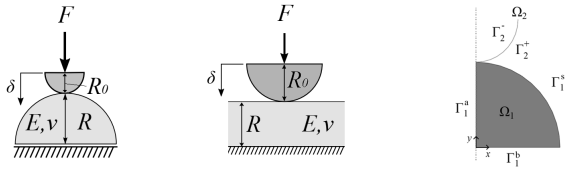


Figure 2. Indentation of a rigid sphere on an elastic sphere (left), on elastic layer (middle); problem domain (right).

If the breast geometry is further simplified to a horizontal layer with thickness R (a flat geometry instead of a spherical one) (Fig. 2 (middle)), the analytical finite strain indentation can be derived as (Vorovich et al. [18]):

$$\frac{\delta}{R_0} = \left(\frac{3(1-\nu^2)F}{4R^2E}\right)^{2/3} - \frac{(1-\nu)DF}{2\pi R R_0 G}, \tag{3}$$

where $D = D(\nu)$ is a function of ν in which $D \to 1.8$ as $\nu \to 0.5$ (incompressible elastic material). Similarly, eq. (3) holds only of an homogeneous material.

For the numerical solution of the mechanical problem, the breast geometry domain is defined as Ω_1 with boundary Γ_1. A rigid indenter with domain Ω_2 and boundary Γ_2 is initially located at the top position of the breast, where the axisymmetric line is located along the y axis as indicated in Fig. 2 (right). The boundary Γ_1 is decomposed into three parts: a bottom Γ_1^b and left (axisymmetric) boundary Γ_1^a, where boundary conditions are applied for displacements u_x and u_y and a displacement δ is applied to the rigid body Ω_2 along the y-axis to simulated the indentation:

$$u_x = 0 \quad \text{on} \quad \Gamma_1^a \quad ; \quad u_y = 0 \quad \text{on} \quad \Gamma_1^b \quad ; \quad u_y = -\delta \quad \text{on} \quad \Omega_2 \tag{4}$$

such that the indenter boundary is decomposed into two parts: an inside Γ_b^- and outside Γ_2^+ portion, where a frictionless non-penetration contact condition is defined between Γ_2^+ and the breast boundary Γ_1^s. According to Graziano et al. [19], the force applied onto the breast varies depending on the operator and their skills, being described as a subjective professional experience. Thus, in this work, a displacement δ of approximately 30% of the radius of the breast structure is considered. The finite element solver Abaqus was used for the numerical simulation of all analyses. Meshes of approximately 2660 axisymmetric triangular linear elements were used to discretize geometry. A static analysis with geometrically nonlinear finite strain formulation was considered, where the contact problem is handled by a penalty contact method.

3 Results

A model verification without cancerous inclusion is presented and the effect of different tumors in subsequently investigated. For all cases, the following values are considered (see Fig. 1): $R = 65$mm (Huang et al. [20]), $R_0 = 20$mm, $t_s = 2$mm, $t_m = 10$mm, while eq. (3) is used to define r_f in order to set different values of breast density ρ. The mechanical properties and considered tumor sizes are indicated in Tab. 1. The breast compression without cancerous inclusion is here investigated considering five different values of breast densities: $\rho = 1.00, \rho = 0.75, \rho = 0.50, \rho = 0.25, \rho = 0.00$. From the breast reaction forces along the direction of applied probe displacements, it is possible to evaluate F. Figure 3 shows the numerical evaluated values of force and displacements for breast density case together with two analytical homogeneous prevision provided by eq. (4) in which the breast composed of only one tissue was considered (values of E for fibroglandular and adipose case).

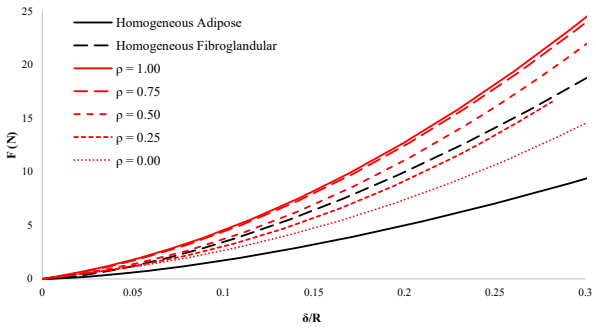


Figure 3. Force-displacement relation for different breast density values.

The adipose tissue has a lower Young' modulus ($E = 15$kPa) when compared to the fibroglandular tissue ($E = 30$kPa), which is stiffer. Therefore, considering the same probe displacement, the adipose tissue will require less force to deform. This can be seen in the curves obtained from the analytical solutions (Figure 3), where the force values for the fibroglandular tissue are higher for the same amount of displacement. Similarly, the same behavior can be observed in the results from the FEA simulations. However, it is important to notice that the values obtained from the simulations using FEA are higher than those obtained by the analytical method. This can be explained by the presence of the skin as an interface between the probe and the other tissues. Because skin has a significantly higher stiffness ($E = 1500$kPa), this directly influences the force necessary to deform the breast.

3.1 Breast Compression with Cancerous Tissue

In order to carry out the analyzes, breast models with different ρ proportions and inclusions with variable diameters and stiffness were considered. The results obtained from the mechanical simulations are illustrated in Fig. 4. The results indicate that for small-sized tumors (Fig. 5, left) there is no significant variation in the compression forces, regardless of the stiffness of the tumor. For larger inclusions (Fig. 5 (middle), 5 (right)), there is a more evident stiffness difference between the forces applied onto the breast. The same observation was reported by another author (da Rocha [6]) in which a different geometric model was analyzed with similar mechanical properties. To observe the strains in the models the Fig. 5 (left) and 5 (right) shows the logarithmic maximum strain field for the 10 mm diameter with E = 33.904 kPa, and 30 mm diameter with E = 111.174 kPa cases. These values represent a benign and malignant cancerous tissue, respectively. If the tumor is of a benign nature, it is softer and tends to produce a lower gradient of strain on its surrounding tissues. However, malignant tumors are stiffer and the strain difference becomes much more evident. Therefore, for small inclusions, the lack of variation throughout the test may lead to false negative results. In such cases, a complementary clinical test might be necessary to assess a more precise conclusion.

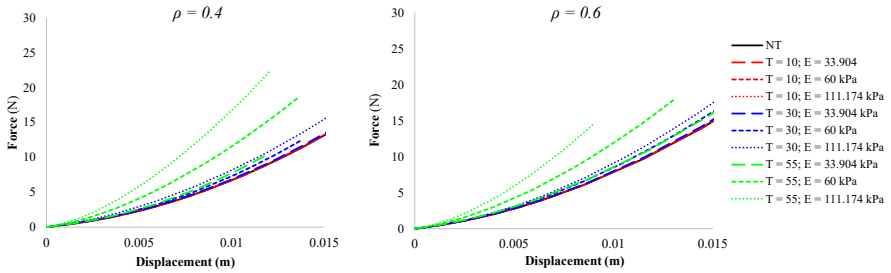


Figure 4. Force-displacement relation for different breast density values with cancerous inclusions.

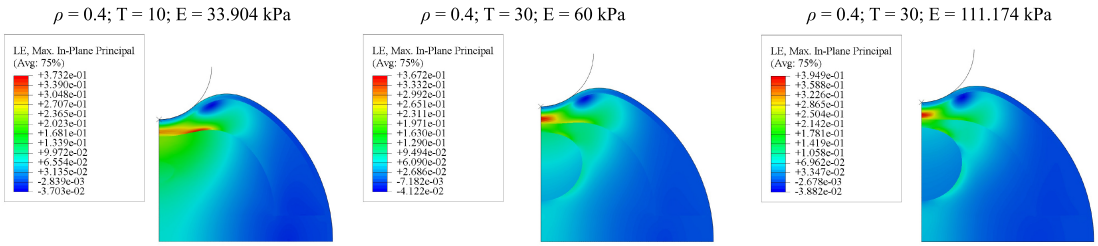


Figure 5. Maximum logarithmic strain field.

Additionally, the relation between applied force and the displacement can be used to determine the tumor's nature. Other authors (Sayed et al. [5]; da Rocha [6]) reported a nonlinear elastic power law behavior where malignant masses exhibits stronger nonlinearity than that observed for the benign case, indicating that malignant masses demonstrate a higher degree of nonlinearity. This pattern was clearly reflected in the strain (and displacement) difference values observed between the masses and the adjacent healthy tissues. In this work, to measure the extent of this nonlinearity, an empirical power-law relationship was employed (Fig. 6), linking the applied force to the strain differences. This relationship was used to fit the estimated data, enabling characterization of how strain differences vary across multiple compression levels. The nonlinear elastic behavior is mathematically represented through the following power-law model (Sayed et al. [21]): $F = M(\Delta\delta)^{1/n}$, where $\Delta\delta$ is the displacement difference between the compression case between the analyzed breast case with a cancerous inclusion (suspected mass) and the compression case without it (healthy soft tissues). The parameters M and n are fitting values obtained from a power law regression procedure, and n is considered to be the main nonlinear parameter characterizing the type of breast mass. If high degrees of the nonlinearity coefficient n is found such that $n > 1$, this displays a malignant behavior (Wellman et al. [22]).

The results obtained for the n values indicate that for the tumor with the smallest diameter (10mm) and lowest Young's modulus (33.904kPa), the benign result is confirmed as expected. The malignant nature of tumors

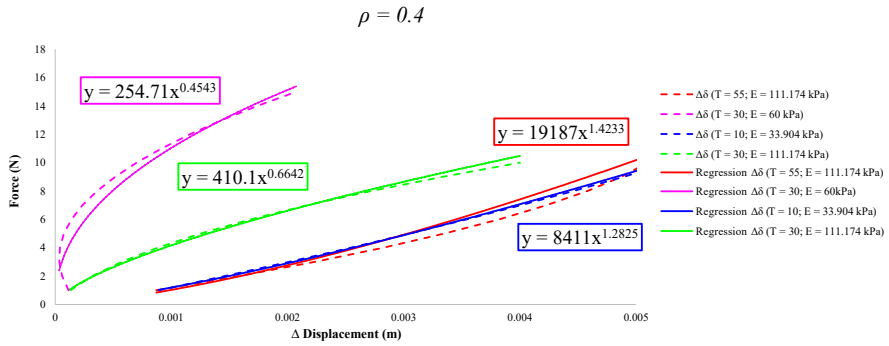


Figure 6. Nonlinearity nature of the cancerous inclusions.

with diameters of 30mm and Young's modulus of E = 60kPa and E = 111.174kPa, respectively, are also confirmed. However, the tumor with the largest diameter (55mm) and highest Young's modulus (111.174kPa) has a n < 1, being a false-negative result. The hypothesis suggested is that: because it has a large dimension and Young's modulus, it is difficult to differentiate with the remaining tissues. Thus, the result obtained from the FEA can be interpreted as if it is a high-density breast. The results obtained by FEA were compared with those provided by da Rocha [6]. As can be seen in Fig. 7, there is a significant distance between the plotted curves. This distance is due to the fact that different geometric models are being compared. Although proportions and mechanical properties of the tissues are the same in both studies, in this work the breast is represented by an elastic hemispherical model, while da Rocha [6] uses an elastic layer model. Since geometry directly influences stiffness, this difference can be observed and explained by the relation obtained by the spherical indentation of an homogeneous elastic sphere (Eq. 2) over an homogeneous elastic layer (Eq. 3). This relation for an homogeneous case with $\rho = 1$ is plotted in Fig 7, showing closer results to those obtained by da Rocha [6].

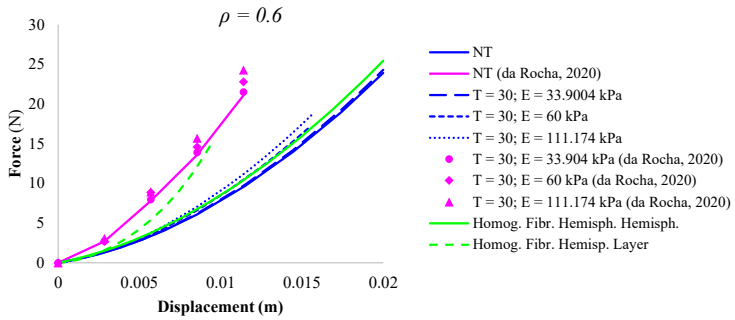


Figure 7. Results comparison.

4 Conclusions

A computational model for simulating the mechanical behavior of breast under compression in a similar condition of the ultrasound elastography clinical test was presented. Different tissues were considered to compose the model and the interaction between a rigid probe indenter was evaluated with three tumor sizes and stiffnesses. The computational simulations were performed using the Finite Element Method with nonlinear considerations. The results indicate that for small sized tumors there is no significant variation in the compression forces, regardless of the stiffness of the tumor. For larger inclusions, there is a more evident stiffness difference between the applied forces onto the breast. This work contributes to the biomechanical understanding of breast compression for cancer detection and potential improvement of clinical elastography tests.

Authorship statement. The authors hereby confirm that they are the sole liable persons responsible for the authorship of this work, and that all material that has been herein included as part of the present paper is either the property (and authorship) of the authors, or has the permission of the owners to be included here.

References

[1] INCA. Estimativa 2023: incidência do câncer no brasil. *Instituto Nacional de Câncer - INCA*, 2022.
[2] INCA. Dados e números sobre o câncer de mama: Relatório anual 2023. *Instituto Nacional de Câncer - INCA*, 2023.
[3] R. G. Barr. *Breast elastography*. Thieme, 1st edition, 2015.
[4] J. Ophir, I. Céspedes, H. Ponnekanti, Y. Yazdi, and X. Li. Elastography: A quantitative method for imaging the elasticity of biological tissues. *Ultrasonic Imaging*, vol. 13, n. 2, pp. 111–134, 1991.
[5] A. M. Sayed, M. A. Naser, A. A. Wahba, and M. A. A. Eldosoky. Breast tumor diagnosisusing finite-elementmodeling based on clinical in vivo elastographic data. *Journal of Ultrasound in Medicine: Official Journal of the American Institute of Ultrasound in Medicine*, vol. 39, n. 12, pp. 2351–2363, 2020.
[6] da A. M. C. Rocha. *Saúde da Mulher: Biomecânica Computacional para Enfrentar os Desafios Clínicos da Mama*. PhD thesis, Faculdade de Engenharia da Universidade do Porto, 2020.
[7] R. G. Barr. Future of breast elastography. *Ultrasonography (Seoul, Korea)*, vol. 38, n. 2, pp. 93–105, 2019.
[8] F. Kallel, M. Bertrand, and J. Ophir. Fundamental limitations on the contrast-transfer efficiency in elastography: An analytic study. *Ultrasound in Medicine Biology*, vol. 22, n. 4, pp. 463–470, 1996.
[9] J. Ophir, S. K. Alam, B. S. Garra, F. Kallel, E. E. Konofagou, T. Krouskop, C. R. B. Merritt, R. Righetti, R. Souchon, S. Srinivasan, and T. Varghese. Elastography: Imaging the elastic properties of soft tissues with ultrasound. *Journal of Medical Ultrasonics*, vol. 29, n. 4, pp. 155–171, 2002.
[10] J. Chen, Y. Sun, Q. Liu, J. Yip, and K.-l. Yick. Construction of multi-component finite element model to predict biomechanical behaviour of breasts during running and quantification of the stiffness impact of internal structure. *Biomechanics and Modeling in Mechanobiology*, vol. 23, n. 5, pp. 1679–1694, 2024.
[11] A. P. Del Palomar, B. Calvo, J. Herrero, J. López, and M. Doblaré. A finite element model to accurately predict real deformations of the breast. *Medical Engineering & Physics*, vol. 30, n. 9, pp. 1089–1097, 2008.
[12] M. Ahangar Darband, E. Najafi Aghdam, and A. Gharibi. Numerical simulation of breast cancer in the early diagnosis with actual dimension and characteristics using photoacoustic tomography. *Archives of Acoustics*, vol. vol. 48, n. No 1, pp. 25–38, 2023.
[13] M. A. Naser, A. M. Sayed, A. A. Wahba, and M. A. A. Eldosoky. Modeling procedures for breast cancer diagnosis based on clinical elastography images. In *2018 13th International Conference on Computer Engineering and Systems (ICCES)*, pp. 671–677, 2018.
[14] M. A. Sak, P. J. Littrup, N. Duric, M. Mullooly, M. E. Sherman, and G. L. G. and. Current and future methods for measuring breast density: A brief comparative review. *Breast Cancer Management*, vol. 4, n. 4, pp. 209–221, 2015.
[15] N. N. A. Nazri, H. Aris, Z. Sauli, and W. M. W. Norhaimi. Assessment of stress and strain on women's breast tissue caused by single round malignant tumor. pp. 020016, Putrajaya, Malaysia, 2020.
[16] J. Said Camilleri, L. Farrugia, S. Curto, D. B. Rodrigues, L. Farina, G. Caruana Dingli, J. Bonello, I. Farhat, and C. V. Sammut. Review of thermal and physiological properties of human breast tissue. *Sensors*, vol. 22, n. 10, pp. 3894, 2022.
[17] I. I. Argatov, X. Jin, and L. M. Keer. Depth-sensing spherical indentation of an elastic sphere on an elastic substrate. *Journal of the Mechanics and Physics of Solids*, vol. 149, pp. 104297, 2021.
[18] I. Vorovich, V. Aleksandrov, and V. Babeshko. Nonclassical mixed problems of the theory of elasticity. *Science, Moscow*, 1974.
[19] L. Graziano, A. G. V. Bitencourt, M. P. Cohen, C. S. Guatelli, M. R. B. Poli, J. A. Souza, and E. F. Marques. Elastographic evaluation of indeterminate breast masses on ultrasound. *Revista Brasileira de Ginecologia e Obstetrícia / RBGO Gynecology and Obstetrics*, vol. 39, n. 02, pp. 072–079, 2017.
[20] S.-Y. Huang, J. M. Boone, K. Yang, N. J. Packard, S. E. McKenney, N. D. Prionas, K. K. Lindfors, and M. J. Yaffe. The characterization of breast anatomical metrics using dedicated breast CT. *Medical Physics*, vol. 38, n. 4, pp. 2180–2191, 2011.
[21] A. Sayed, G. Layne, J. Abraham, and O. Mukdadi. Nonlinear characterization of breast cancer using multi-compression 3d ultrasound elastography in vivo. *Ultrasonics*, vol. 53, n. 5, pp. 979–991, 2013.
[22] P. S. Wellman, R. D. Howe, and K. A. Kern. Breast tissue stiffness in compression is correlated to histological diagnosis, 1999.